Title:

Sea-level rise due to polar ice-sheet mass loss during past warm periods

Authors:
A. Dutton[1*], A. E. Carlson[2], A. J. Long[3], G. A. Milne[4], P. U. Clark[2], R. DeConto[5], B. P. Horton[6,7], S. Rahmstorf[8], M. E. Raymo[9]

[1] Department of Geological Sciences, University of Florida, USA.
[2] College of Earth, Ocean, and Atmospheric Sciences, Oregon State University, USA.
[3] Department of Geography, Durham University, UK.
[4] Department of Earth Sciences, University of Ottawa, Canada.
[5] Department of Geosciences, University of Massachusetts, USA.
[6] Department of Marine and Coastal Sciences, Rutgers University, USA.
[7] Earth Observatory of Singapore, Nanyang Technological University, Singapore.
[8] Potsdam Institute for Climate Impact Research, Germany.
[9] Lamont-Doherty Earth Observatory, Columbia University, USA.

*Correspondence to: adutton@ufl.edu

1-pg SUMMARY:

Background

Although thermal expansion of seawater and melting of mountain glaciers has dominated global mean sea level (GMSL) rise over the last century, mass loss from the Greenland and Antarctic ice sheets is expected to exceed other contributions to GMSL rise under future warming. To better constrain polar ice-sheet response to warmer temperatures, we draw upon evidence from interglacial periods in the geologic record that experienced warmer polar temperatures and higher GMSLs than present. Coastal records of sea level from these previous warm periods demonstrate geographic variability due to the influence of several geophysical processes that operate across a range of magnitudes and timescales. Inferring GMSL and, thus, ice-volume changes from these reconstructions is non-trivial and generally requires the use of geophysical models.

Advances

Interdisciplinary studies of geologic archives have ushered in a new era of deciphering magnitudes, rates and sources of sea-level rise. Advances in our understanding of polar ice-sheet response to warmer climates have been made through an increase in the number and geographic distribution of sea-level reconstructions, better ice-sheet constraints, and the recognition that several geophysical processes cause spatially complex patterns in sea level. In particular, accounting for glacial isostatic processes helps to decipher spatial variability in coastal sea-level records and has reconciled a number of site-specific sea-level reconstructions for warm periods that have occurred within the past several hundred thousand years. This enables us to infer that during recent interglacial periods, small

increases in global mean temperature and just a few degrees of polar warming relative to the pre-Industrial period resulted in ≥6 meters of GMSL rise. Mantle-driven dynamic topography introduces large uncertainties on longer timescales, affecting reconstructions for time periods such as the Pliocene (~3 million years ago), when atmospheric CO_2 was ~400 ppm, similar to that of the present. Both modeling and field evidence suggest that polar ice sheets were smaller during this time period, but because dynamic topography can cause tens of meters of vertical displacement of at the Earth's surface on million-year timescales and uncertainty in model predictions of this signal are large, it is currently not possible to make a precise estimate of peak GMSL during the Pliocene.

Outlook

Our present climate is warming to a level associated with significant polar ice-sheet loss in the past, but a number of challenges remain to further constrain ice-sheet sensitivity to climate change using paleo-sea level records. Improving our understanding of rates of GMSL rise due to polar ice-mass loss is perhaps the most societally relevant information the paleo record can provide, yet robust estimates of rates of GMSL rise associated with polar ice-sheet retreat and/or collapse remain a weakness in existing sea-level reconstructions. Improving existing magnitudes, rates, and sources of GMSL rise will require a better (global) distribution of sea-level reconstructions with high temporal resolution and precise elevations, and should include sites close to present and former ice sheets. Translating such sea-level data into a robust GMSL signal demands integration with geophysical models, which in turn can be tested through improved spatial and temporal sampling of coastal records.

Further development is needed to refine estimates of past sea level from geochemical proxies. In particular, paired oxygen isotope and Mg/Ca data are currently unable to provide confident, quantitative estimates of peak sea level during these past warm periods. In some GMSL reconstructions, polar ice-sheet retreat is inferred from the total GMSL budget, but identifying the specific ice-sheet sources is currently hindered by limited field evidence at high latitudes. Given the paucity of such data, emerging geochemical and geophysical techniques show promise for identifying the sectors of the ice sheets that were most vulnerable to collapse in the past and perhaps will be again in the future.

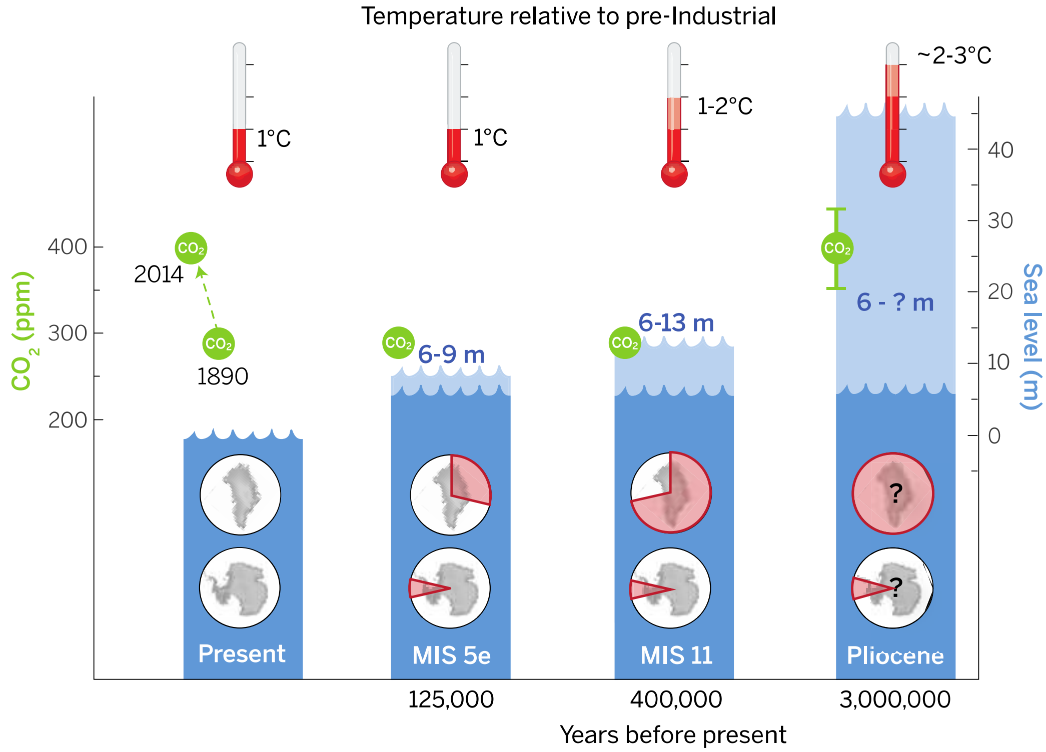

Figure 1.

Peak global mean temperature, atmospheric CO_2, maximum global mean sea level (GMSL), and source(s) of meltwater. Light blue shading indicates uncertainty of GMSL maximum. Red pie charts over Greenland and Antarctica denote fraction (not location) of ice retreat.

Title:

Sea-level rise due to polar ice-sheet mass loss during past warm periods

Authors:

A. Dutton[1*], A. E. Carlson[2], A. J. Long[3], G. A. Milne[4], P. U. Clark[2], R. DeConto[5], B. P. Horton[6,7], S. Rahmstorf[8], M. E. Raymo[9]

[1] Department of Geological Sciences, University of Florida, USA.
[2] College of Earth, Ocean, and Atmospheric Sciences, Oregon State University, USA.
[3] Department of Geography, Durham University, UK.
[4] Department of Earth Sciences, University of Ottawa, Canada.
[5] Department of Geosciences, University of Massachusetts, USA.
[6] Department of Marine and Coastal Sciences, Rutgers University, USA.
[7] Earth Observatory of Singapore, Nanyang Technological University, Singapore.
[8] Potsdam Institute for Climate Impact Research, Germany.
[9] Lamont-Doherty Earth Observatory, Columbia University, USA.

*Correspondence to: adutton@ufl.edu

Abstract:

Interdisciplinary studies of geologic archives have ushered in a new era of deciphering magnitudes, rates and sources of sea-level rise from polar ice-sheet loss during past warm periods. Accounting for glacial isostatic processes helps to reconcile spatial variability in peak sea level during Marine Isotope Stages (MIS) 5e and 11, when the global mean reached 6-9 m and 6-13 m higher than present, respectively. Dynamic topography introduces large uncertainties on longer timescales, precluding robust sea-level estimates for intervals such as the Pliocene. Present climate is warming to a level associated with significant polar ice-sheet loss in the past. Here we outline advances and challenges involved in constraining ice-sheet sensitivity to climate change using paleo-sea level records.

One sentence summary: Advances in reconstructions of past sea level reveal high sensitivity of polar ice sheets to small warming.

Main text:

Global mean sea level (GMSL) has risen over the past century largely in response to global warming (~0.19 m rise in GMSL between 1901 and 2010) (*1*). The response to global warming includes thermal expansion of ocean water as well as mass loss from glaciers and ice sheets, all of which increase the volume of water in the ocean and, thus, cause a sea-level rise. Recent GMSL rise has been dominated by thermal expansion and glacier loss, which collectively explain ~75% of the observed rise since 1971 (*1*). The contribution from mass loss from the Greenland (GrIS) and Antarctic (AIS) ice sheets has increased since the early 1990s, comprising ~19% of the total observed rise in GMSL between 1993-2010 (*1*), and is expected to exceed other contributions under future sustained warming (e.g., *2*). Estimates from short, recent time periods—though not as robust as analyses of longer records due to the dominance of interannual variability—suggest that polar ice-sheet loss may now comprise as much as ~40% of the total observed rise in GMSL between 2003-2008 (*3, 4*).

These same processes contributed to higher-than-present sea levels in the past when global mean temperature was warmer than the pre-Industrial period (before 1750). However, because mountain glaciers and thermal expansion can only explain ~1-1.5 m of GMSL rise for the 1-3 °C warming associated with these periods (*5, 6*), evidence for former GMSL exceeding this amount requires a contribution from the GrIS and/or AIS. Understanding how polar ice sheets lost mass and contributed to sea-level rise during past warm periods can provide insights into their sensitivity to climate change as well as constrain process-based models used to project ice-sheet response to future climate change.

Many studies have used data and/or models to determine the sensitivity of ice sheets to changes in temperature or atmospheric CO_2 over long timescales (*2, 7-12*). Given the recent increases in greenhouse gases (GHGs) and global mean temperature, the present ice sheets are out of equilibrium with the climate, raising important questions regarding their potential future contribution to sea-level rise: (i) What is the equilibrium sea-level rise for a given warming scenario? (ii) How quickly will the GrIS and AIS respond to present and future radiative forcing and associated warming and what will be the accompanying rates of sea-level change? (iii) What are the source regions of the ice-mass loss, a factor that will strongly influence the geographic pattern of future sea-level change (*1, 2, 13*)?

To address these questions, we examine how our understanding of ice-sheet response during past warm periods is evolving through the progressive integration of several disciplines. In particular, we consider observational evidence of paleo sea levels and ice-sheet reconstructions, with climate, ice-sheet, and solid Earth models. For each time period, we identify key geophysical signals that must be quantitatively estimated and removed from relative sea level (RSL; refers to the local height of sea level) records in order to infer past changes in GMSL (Text Box 1). Finally, we review the state of knowledge regarding the magnitudes, rates, and sources of sea-level rise during several of the most prominent interglacial peaks of the last three million years, including the Mid-Pliocene warm period (MPWP, ~ 3 million years ago), MIS 11 (~400 thousand years ago (ka)), and MIS 5e (~125 ka) (Fig. 1).

Mid-Pliocene Warm Period (~3.2 to 3.0 million years ago)

The MPWP comprises a series of orbitally paced (41-thousand year (ky)) climate cycles associated with atmospheric CO_2 in the range of 350-450 ppm (*14, 15*). Peak global mean temperatures derived from general circulation model simulations average 1.9-3.6 °C warmer than pre-Industrial (*16*). Some Arctic temperature reconstructions indicate warming of 8 °C or more while some Southern Ocean records suggest warming of 1-3 °C (*17*). However, these temperature estimates are uncertain and, in some cases, may not correlate precisely to the MPWP time interval. Both modeling and field evidence suggest that polar ice sheets were smaller during the MPWP, but constraints on the magnitude of GMSL maxima during the warm extremes as inferred from RSL reconstructions are highly uncertain (*18*).

In the Southern Hemisphere, the West Antarctic Ice Sheet (WAIS) experienced multiple retreat and advance phases during the Pliocene (*19*). Studies of ice-rafted debris (IRD) suggest that portions of the East Antarctic Ice Sheet (EAIS) experienced retreat during parts of the early to middle Pliocene (*20*), apparently paced by precessional (23-kyr) cycles (*21*). In the Northern Hemisphere, there are no firm observational constraints on changes in the size of the MPWP GrIS. Ice-sheet models, on the other hand, simulate retreat in both Greenland (*22*) and Antarctica (*12*) in response to imposed Pliocene climate forcing, raising GMSL by ~7 m and ~6 m, respectively.

Many early studies of Pliocene coastal records considered the Earth to be rigid and thus, inferred a uniform GMSL rise across a wide range of elevations (+15-60 m, see Table 1 in (*18*)). Some studies attempted to correct individual RSL records for the influence of local tectonics or subsidence (*23-27*). More recently, Raymo et al. (*18*) corrected Pliocene RSL observations for the effects of GIA, but the global variability in the elevation of observed shorelines remains substantial, ranging over tens of meters. This is thought to be due to the influence of dynamic topography, as well as to uncertainties in the elevation and age of the shoreline features (*18, 28, 29*). Improvements in model parameters for GIA and dynamic topography and in dating of coastal records are thus needed to better constrain estimates of Pliocene sea level from coastal records.

The amplitude of negative excursions in benthic $\delta^{18}O$ records during the MPWP (~0.4‰ relative to the Holocene) (Fig. 1) may imply higher GMSL than today, but extracting the ice-volume signal from the $\delta^{18}O$ calcite record remains a challenge. Typical analytical errors in $\delta^{18}O$ measurements translate to large uncertainties in sea level (~ ±10 m). Moreover, inferring ice volume requires that the contribution of seawater temperature and hydrography to the benthic $\delta^{18}O$ signal is known. The Mg/Ca of the benthic calcite record can be used to isolate the temperature portion of the corresponding $\delta^{18}O$ signal, but uncertainties in calibration (*30, 31*), carbonate ion saturation (*32*), diagenesis of calcite (*33*), and long-term seawater Mg/Ca variability (*34*) are significant. Until these effects are better understood and able to be isolated, the $\delta^{18}O$ proxy records will continue to be plagued by errors as large as the signal we are seeking. In light of these considerations, the Miller et al. (*24*) peak GMSL estimate of 21 ± 10 m at the end of the MPWP (~2.95 Ma) that is based on evidence from non-GIA corrected coastal records, benthic $\delta^{18}O$ (*35*), and paired $\delta^{18}O$-Mg/Ca records probably carries more uncertainty than the quoted range.

Marine isotope stage 11 (~424,000-395,000 years ago)

Marine isotope stage (MIS) 11 was an unusually long interglacial period (~30 kyr) with a highly uncertain global average temperature (estimates range from slightly cooler than MIS 5e (see below) (*36, 37*) up to ~2 °C warmer than pre-Industrial (*38*)) and atmospheric CO_2 peaking at 286 ppm (similar to pre-Industrial values) (*39*). Limited proxy data indicate Arctic summer maximum air and sea surface temperatures reaching up to 4 and 9 °C warmer, respectively, than peaks attained during MIS 1 or 5e (*40, 41*). Antarctic ice-core analyses indicate temperatures ~2.6 °C warmer than pre-Industrial (*42*). Climate models forced by insolation and GHG concentrations during MIS 11, however, simulate only slightly warmer global mean temperatures (~0.1 °C) than for MIS 1 (*38, 43*). Hence, if the limited proxy data are correct in implying enhanced warmth in the polar regions, the underlying cause of the warmer climates is unresolved.

Reconstructions of MIS 11 GMSL suggest that it was higher than present. Several records document at least partial retreat of the GrIS during MIS 11, suggesting it contributed to higher GMSL. Pollen in marine records offshore of southeast Greenland indicate the development of spruce forest over parts of now-ice-covered regions (*44*). Likewise, biomolecules from the base of the Dye-3 ice core indicate a forested southern Greenland that could be from MIS 11, although the age of these molecules is uncertain (*45*). A cessation of ice-sheet eroded sediment discharge and IRD suggests ice-margin retreat from the southern Greenland coast (*46*), whereas continued IRD deposition in the northeast demonstrates the persistence of marine-terminating ice over northeastern Greenland (*47*). Comparison of these constraints with ice-sheet models suggests that the GrIS could have contributed 4.5-6 m to GMSL rise above present (*46*). Higher GMSL estimates thus require an Antarctic contribution, but few geologic constraints on AIS history exist for MIS 11 (*48*).

Early work on interpreting MIS 11 coastal records assumed a geographically uniform GMSL change, with sea-level estimates ranging from -3 m (*49*) to +20 m (*50*). If the records are all the same age, the large range may largely reflect geographic variability in the RSL signal associated with GIA and dynamic topography (Box 1). For example, when corrected for GIA, MIS 11 RSL in the Bermuda and Bahamas regions (~20 m above present) suggests a peak GMSL of only 6-13 m above present (*51*), a level that would require loss of the GrIS and/or sectors of the AIS. This estimate is consistent with the 8-11.5 m estimate based on paleoshorelines in South Africa that have been corrected for GIA effects and local tectonic motion (*52, 53*). Overall, multiple lines of evidence would seem to agree that GMSL was 6-13 m higher near the end of MIS 11.

By comparison, paired $\delta^{18}O$ – Mg/Ca measurements of benthic foraminifera suggest GMSL during MIS 11 in excess of 50 ± ~20 m above present (*31, 54*), although as with the MPWP reconstructions, the uncertainties on these estimates may be much larger. On the other hand, the Red Sea planktic $\delta^{18}O$ record suggests RSL reached just above present (1 ± 12 m at 2σ) (*55, 56*). Additional contributions from GIA and possibly also from dynamic topography to the sill depth of the Red Sea over the last several hundred kyr that are not captured in the present reconstruction could impart additional uncertainties. The large uncertainty and lack of agreement associated with all of these $\delta^{18}O$-based records points to the difficulty in using them to tightly constrain peak GMSL during previous warm periods.

Marine isotope stage 5e (~129,000–116,000 years ago)

We consider the time interval of MIS 5e when GMSL was above present (~129-116 ka) (*8, 57*). Relative to the pre-Industrial period, model simulations indicate little global average temperature change during MIS 5e, while proxy data imply ~1 °C of warming, but with possible spatial and temporal sampling biases (*58*). Greenland temperatures peaked between ~5-8 °C above pre-Industrial (*59, 60*) and Antarctic temperatures were ~3-5 °C warmer (*42*).

Shorelines that developed during the MIS 5e sea-level highstand are the best-preserved and most geographically widespread record of a higher-than-present GMSL during a previous warm period. Recent global compilations of RSL data combined with GIA modeling indicate that peak GMSL was higher than the previous long-standing estimate (4-6 m), in the range of ~6-9 m above present (*61, 62*), in agreement with site-specific, GIA-corrected coastal records in the Seychelles at 7.6 ± 1.7 m (*63*) and in Western Australia at 9 m (no uncertainty reported) (*64*) above present (Fig. 3). The Red Sea planktic $\delta^{18}O$ record places peak RSL values during MIS 5e at 6.7 ± 3.4 m (maximum probability with 95% probability envelope) (*65*). Detailed GIA corrections for the temporal evolution of the hydraulic geometry of the Red Sea during MIS 5e are not applied to this planktic $\delta^{18}O$ record, and could change the peak value by a few meters (*66*). Paired benthic $\delta^{18}O$-Mg/Ca data (*31, 54*) reflect high uncertainty and poor agreement for peak GMSL when compared to the coastal records (Fig. 4).

The 3 m uncertainty range in peak GMSL derived from coastal records (i.e., ~6-9 m) presents a challenge when assessing relative GrIS and AIS contributions. Ice-core and marine records show that the GrIS was smaller than present during MIS 5e, with substantial (but not complete) retreat of the southern sector at the same time as peak GMSL ~122-119 ka (*60, 67*). Recent modeling studies suggest that total GrIS mass loss was between 0.6-3.5 m (Fig. 3, and references therein). With thermal expansion and melting of mountain glaciers contributing up to ~1 m rise (*5, 68*), an additional contribution is required from the AIS to explain peak GMSL during MIS 5e. However, direct evidence for AIS retreat at this time is lacking, with only some poorly dated records that suggest that WAIS retreated during some previous interglacial periods, including possibly MIS 5e (*69*).

The primary means of establishing an accurate and precise chronology for MIS 5e sea level is through U-Th dating of fossil corals that lived near the sea surface. Existing chronologies suggest regional differences in the timing of peak MIS 5e RSL. In some cases, this reflects variable diagenesis that causes open-system conditions in the corals with respect to U and Th isotopes (e.g., *70*). However, differences in timing may also be real and reflect the spatially variable influence of GIA (*61*). Most studies suggest that peak GMSL occurred sometime after ~125 ka, usually in the range of ~122-119 ka (*64, 71-74*), but the timing of AIS versus GrIS contributions to maximum GMSL remains unresolved.

Differences in RSL reconstructions from site to site yield a range of interpretations about the evolution of GMSL during the MIS 5e highstand, including: (i) a stable sea level (*57*); (ii) two peaks separated by an ephemeral drop in sea level (*72, 73*); (iii) a stable sea level followed by a rapid sea-level rise (*64, 71*); and (iv) three to four peaks in sea level reflecting repeated sea-level oscillations (*74, 75*). As yet, no consensus exists regarding this suite of scenarios, but robust sedimentary evidence from multiple coastal sites argues for at least one and possibly several meter-scale sea-level oscillations during the course of the highstand (e.g., *64, 71, 72, 73, 76*). These data suggest dynamic behavior of polar ice sheets at a time when global mean temperature was similar to present. It is not clear whether such variability was driven by one unstable ice-sheet sector or by differences in the phasing of ice-mass changes in multiple ice-sheet sectors across the duration of MIS 5e.

Estimated rates of sea-level change associated with these oscillations range from 1-7 m kyr^{-1} (*74, 75, 77*). Resolving rates on shorter timescales is hindered by the precision of the dating and RSL reconstruction methods. Even the m kyr^{-1} rates listed above are highly uncertain if one incorporates a full consideration of observational errors. For example, MIS 5e reefs in the Bahamas have uncertainties in coral paleo-water depths of >5 m (based on the assumed depth range of *Acropora palmata*) or more (for the *Montastrea sp.* and *Diploria sp.*), which are similar in magnitude to the inferred change in sea level (4-6 m) (*72, 74*). As another example, meter-scale RSL fluctuations during the MIS 5e highstand inferred from the Red Sea planktic $\delta^{18}O$ record are not replicated between the two cores used in the analysis and the variability largely falls within the reported uncertainty, so it is not possible to reject the null hypothesis that RSL was stable based on this record (*75*). Thus, despite the clear sedimentary evidence for sea-level variability in during MIS 5e, associated rates of GMSL change remain poorly resolved.

The Holocene (11,700 years ago to present)

Global mean temperatures during the Holocene have ranged from ~0.75 °C warmer (from ~9.5-5.5 ka) than pre-Industrial temperatures (*78*) to pre-Industrial levels (*79*). While this temperature reconstruction is relatively well constrained by proxy data, we note that models simulate a warming trend through the Holocene, which may be an indication of uncertainty in the reconstructions, the models, or both (*80*).

The Holocene has the most abundant and highly resolved RSL reconstructions in comparison to previous interglacial periods (Fig. 2). In addition, the history of ice-sheet retreat is relatively well constrained, particularly in the Northern Hemisphere. Detailed sea-level reconstructions from the last few millennia are important for constraining the natural variability in sea level and, thus, providing context for evaluating current and future change (*1, 81*).

GMSL was ~60 m lower than present at the beginning of the Holocene, due largely to the remaining Scandinavian and Laurentide ice sheets as well as a greater-than-present AIS volume. Rates of GMSL rise slowed by ~7 ka following the final deglaciation of the Laurentide Ice Sheet—from ~15 m kyr^{-1} between ~11.4-8.2 ka to ~1 m kyr^{-1} or less for the remainder of the pre-Industrial Holocene (*82*). Only a few meters of ice-sheet loss occurred between ~7 and ~2 ka (*82, 83*), which is thought to be dominated by loss from the AIS (*84, 85*). Field data and ice-sheet models suggest that the GrIS was smaller than present during the early to middle Holocene thermal optimum (9.5-5.5 ka) (*86, 87*), and began to re-advance during the cooler Neoglacial period (<5 ka), reaching its maximum extent in many places during the Little Ice Age and causing a GMSL lowering of <0.2 m (*88*).

Over the last ~7 kyr, RSL has fallen in many near-field areas that were formerly covered by major ice sheets because of glacial isostatic rebound (Fig. 2a), while RSL in intermediate- and far-field regions reflects changes in GMSL, proglacial forebulge collapse, and hydro-isostatic loading (*89, 90*), with deltaic regions being further influenced by compaction (Fig. 2b-d). Equatorial and Southern Hemisphere RSL reconstructions record a mid-Holocene highstand at ~6 ka of a few decimeters to several meters (*91, 92*) (Fig. 2e-h) that is a consequence of the GIA effect known as equatorial siphoning (*89, 90*).

Sea-level reconstructions from salt marshes bordering the North Atlantic region reveal regional decimeter-scale variability on multi-decadal to millennial timescales over the last ~2 ka (*93, 94*) (Fig. 2i) that reflect ice-sheet loss and coupled atmosphere-ocean variability (*95*). Late-Holocene ice-margin reconstructions for the AIS suggest little change (*84, 85, 96*), while those for the GrIS suggest general advance (*86-88*). The clearest signal in geological and long tide gauge records is the transition from low rates of change during the last ~2 ka (order tenths of mm yr^{-1}) to modern rates (order mm yr^{-1}) in the late 19th to early 20th centuries, although the spatial manifestation of this change is variable (*1, 81*).

Discussion and Future Challenges

Recent interdisciplinary studies on sea-level and ice-sheet change during previous warm periods confirm that there is a strong sensitivity of polar ice-sheet mass loss (and associated sea-level rise) to higher insolation forcing and polar temperatures and similar or higher GHG forcing (Fig. 4). This understanding of polar ice-sheet response to climate change has improved considerably through an increase in the number and geographic distribution of RSL reconstructions, better ice-sheet constraints, and the recognition that several geophysical processes cause spatially complex patterns across timescales spanning tens to millions of years (Figs. 1-2). Spatial variability in Holocene RSL from GIA has long been recognized (*89*), but widely disparate estimates of the magnitude of GMSL change associated with any given previous warm period have only recently been documented as similarly reflecting the spatial variability in RSL resulting from GIA and dynamic topography (e.g., see MIS 5e estimates in Fig. 3).

Despite the many advances in our understanding of GMSL during past warm periods, a number of challenges remain. Foremost among these is the need to continue to improve the accuracy and precision of the age and elevation of RSL indicators. In particular, now that we recognize that time-dependent GIA effects will affect the elevation of shorelines depending on whether they formed early or late in the interglacial period, improving chronologies to resolve the timing of observations during RSL highstands becomes all that much more critical to inferring the GMSL signal (*51, 61*). Although the precision of U-Th dating has improved, complications related to open-system diagenesis and former seawater U-isotope composition continue to limit precision and accuracy of marine carbonate U-Th ages (see review by *97*).

Translating site-specific data into a global context requires better constraints on the properties of the solid Earth that strongly influence RSL on long timescales, especially the viscosity and density structure of the mantle. Increased spatial and temporal density of past RSL and ice-sheet margins will improve ice and Earth models, while use of 3-D GIA models may improve predictions in areas where lateral heterogeneities are important (*98*).

Determining equilibrium GMSL for different forcing scenarios using paleo data requires consideration of factors beyond understanding the peak value of GMSL, polar (or global) temperature, or atmospheric CO_2 during a given time period. Given lags in the climate system, simple correlation between such climate parameters can be misleading because the extremes may not be synchronous over a 10-kyr long interglacial period. Peak temperatures attained during previous warm periods may also be dependent upon the length of the interglacial period (*41, 46*), suggesting that warm periods lasting several kyr may not represent equilibrium conditions for the climate-cryosphere system. Moreover, ice sheets in different hemispheres may not respond in phase.

In the case of MIS 11 and 5e, warm climates and higher GMSL resulted largely from orbital forcing that changes the intensity of solar insolation at high latitudes. Insolation forcing is quite different from the relatively uniform global forcing of increased atmospheric CO_2 that will influence future sea levels. Furthermore, regional sea and air temperatures exert the most direct influence on mass loss from a polar ice sheet, suggesting that past global mean temperature may not be the best predictor for past GMSL. More detailed regional climate reconstructions thus represent an additional target to improve understanding of the climatic forcing required for specific ice-sheet response scenarios. Improved chronological frameworks are also required that can directly relate sea-level and climate reconstructions, particularly to facilitate comparisons between reconstructions that rely on radiometric versus orbitally tuned chronologies.

In the following, we summarize our current understanding of magnitudes, rates, and sources of sea-level change during warm periods and their associated uncertainties, and conclude with the recommendation to develop comprehensive databases that will be required to optimally capture the temporal and spatial variability of past high sea levels and their sources.

Magnitudes of GMSL Rise: The best agreement in the magnitude of peak GMSL is between multiple GIA-corrected coastal records for MIS 5e and 11, but the uncertainty introduced from the combined influence of GIA and dynamic topography going farther back in time presently precludes us from placing a firm estimate on GMSL during the MPWP interglacial peaks. Given the constraints from existing data and models of MPWP temperatures and ice-sheet reconstructions combined with the evidence for stronger GHG forcing, we hypothesize that MPWP sea levels would have exceeded those attained during MIS 11 and 5e. This provides a lower bound of +6 m with the distinct potential for higher GMSL, particularly if the GrIS, WAIS, and EAIS experienced simultaneous mass loss. This hypothesis should be tested in the context of additional data and modeling constraints.

In comparison to GIA-corrected coastal records, paired $\delta^{18}O$-Mg/Ca records have greater uncertainty, and in several cases have poor accuracy, suggesting that the current state of these geochemical methods makes them unable to provide confident, quantitative estimates of peak GMSL during these periods (Fig. 4). The planktic $\delta^{18}O$ from the Red Sea (*15, 75, 84*) is an innovative approach to overcoming some of the limitations of the benthic $\delta^{18}O$ or paired $\delta^{18}O$-Mg/Ca methods and remains one of the most valuable, semi-continuous records of sea-level change across century to millennial timescales. However, it carries uncertainties that are common to both the coastal reconstructions (such as GIA corrections) as well as the other $\delta^{18}O$-based reconstructions, some of which will magnify farther back in time. Targeted GIA modeling of the Red Sea basin, in particular to derive isostatic corrections for the Hanish Sill during these interglacial highstands, would be a valuable undertaking towards using this reconstruction to interpret GMSL.

Rates of GMSL Rise: Rates of sea-level change for previous warm periods when sea level was higher than present range from highly uncertain to completely unconstrained depending on the time period, yet this is perhaps the most societally relevant information the paleo record can provide for predicting and adapting to future sea-level change. MIS 5e holds the greatest potential for information on past rates of sea-level change in a world with higher GMSL. While MIS 5e sea-level oscillations appear abrupt in the sedimentary record, uncertainties in dating and interpretation of RSL markers have prevented precise quantification of this abruptness beyond an indication that GMSL rose (and fell) one to several meters over one to a few kyr (e.g., *74*). Hence, deriving rates of interest on societal timescales (cm yr^{-1}, m $century^{-1}$), such as can be achieved in Holocene reconstructions, remains a primary challenge.

Resolving meter-scale sea-level variability during the MIS 5e highstand will require precise chronologies and stratigraphy of sea-level indicators as well as improved precision in the vertical uncertainties of RSL indicators. Coastal geomorphological features, while compelling, are difficult to date. Fossil corals can potentially provide robust chronologies, if challenges associated with the interpretation of post-depositional alteration of U-Th isotope measurements can be overcome (*97*). Further, fossil corals are usually associated with significant vertical uncertainties in their paleowater depth. Future improvements on existing paleowater depth estimates of fossil corals will require integration of paleoenvironmental information, including assemblages of reef biota, and a more quantitative understanding of the depth distribution of modern corals and associated reef biota (*99*).

The rate of GMSL rise associated Northern Hemisphere ice-sheet retreat during the last deglaciation is often cited as providing an upper bound for potential future GMSL rise (e.g., >4 m $century^{-1}$ during meltwater pulse 1A: *100*). The nature and forcing of that retreat, however, is expected to be significantly different to that of the warm-climate polar ice sheets and thus not directly analogous. Nevertheless, there are aspects of past sea-level changes during glacial maxima or during deglacial transitions that are relevant to understanding interglacial GMSL change. For example, recent modeling identified a identified a positive feedback involving 'saddle collapse' of the Laurentide Ice Sheet melting that is capable of delivering a substantial influx of meltwater as a possible mechanism contributing to MWP-1A (*101*). Saddle collapse between the southern and northern domes of the GrIS may be important for driving smaller scale, but rapid GMSL change during warm interglacial periods. Similarly, there is increasing evidence that ocean thermal forcing played an important role in destabilizing late-Pleistocene ice sheets (e.g., *102*), similar to what is projected for the future.

Constraining the total volume and geographic extent of grounded ice during the Last Glacial Maximum (LGM), in particular, is an important parameter for GIA model predictions of RSL across all time periods, including the present and past interglacial periods (e.g., *18*). Improved constraints on LGM ice volume will also influence the quantification of GMSL changes based on benthic $\delta^{18}O$ reconstructions as well as paired $\delta^{18}O$-Mg/Ca reconstructions. However, there are presently few far-field sites with RSL histories that can be used to constrain the LGM. We note that an ~120 m-below-present GMSL during the LGM has long been held as conventional wisdom, yet several recent (and some earlier) GIA studies put the estimate in the range of 130-134 m below present (Fig. S1). Because the total volume and extent of the LGM ice sheets is a sensitive parameter for GIA model predictions, improving our understanding of glacial ice loads will influence our interpretations of rates and magnitudes of interglacial GMSL.

Sources of GMSL Rise: Two approaches show great promise for identifying and quantifying the contribution of individual ice sheets that retreated during previous warm periods: geochemical provenance in marine sediments (*20, 46, 67*) and sea-level fingerprinting (*103*). Existing evidence points to southern Greenland as the most susceptible sector of the GrIS to warmer-than-present temperatures (*46, 67*), although some models predict retreat in the north and others in the south. In Antarctica, compelling sedimentary (*19, 21*) and modeling (*12, 104*) evidence suggests that repeated retreat-advance cycles of the WAIS occurred during the Pliocene and early Pleistocene, but little direct evidence constrains changes in the AIS during more recent intervals, including MIS 11 and 5e and the Holocene. Marine-based portions of the EAIS may be just as vulnerable as the WAIS and should be equally considered as contributors to past sea-level change (*105*).

Improving our understanding of individual polar ice-sheet contributions to GMSL is a key challenge. An important uncertainty for future projections of the GrIS is the threshold temperature beyond which it undergoes irreversible retreat, with current estimates ranging from 1-4°C above pre-Industrial temperatures (*1*). Improved estimates of GrIS loss for a given local or global temperature increase during past warm periods will thus provide a critical constraint on this threshold. For the AIS, the key challenge involves determining which marine-based sectors are most vulnerable to collapse, and identifying the forcing (atmospheric or oceanic) that would trigger such events. Paleo-constraints on past ice-sheet mass loss and forcings will be of particular value for validation of coupled ice sheet-climate models.

Recommendations:

Addressing outstanding questions and challenges regarding rates, magnitudes, and sources of past polar ice-sheet loss and resulting sea-level rise will continue to require integration of ice-sheet, sea-level, and solid Earth geophysical studies with good spatial distribution of well-dated RSL records to capture the magnitude of RSL variability across the globe. Such synoptic analyses will need a sufficiently sophisticated cyberinfrastructure to enable data sharing, transparency, and standardization of sea-level and ice-sheet paleo data that are derived from multiple and diverse sub-disciplines. Where sufficiently resolved, such data can then be used to identify sources of meltwater through their sea-level fingerprints and refine estimates of GMSL change (*103, 106*). Near-field records of ice-sheet extent and climate will also be essential in identifying the sources and forcing mechanisms responsible for sea-level change. Most importantly, transcending conventional paradigms of sea-level reconstructions and adopting the concept of geographic variability imparted by dynamic physical processes will continue to lead to significant advances in our understanding of GMSL rise in a warming world.

References and Notes:

1. J. A. Church *et al.*, in *Climate Change 2013: The Physical Science Basis. Contribution of Working Group I to the Fifth Assessment Report of the Intergovernmental Panel on Climate Change* T. F. Stocker *et al.*, Eds. (Cambridge University Press, Cambridge, 2013), pp. 1137-1216.
2. A. Levermann *et al.*, The multimillennial sea-level commitment of global warming. *Proceedings of the National Academy of Sciences* **110**, 13745 (2013).
3. A. Cazenave *et al.*, Sea level budget over 2003–2008: A reevaluation from GRACE space gravimetry, satellite altimetry and Argo. *Global and Planetary Change* **65**, 83 (2009).
4. V. Helm, A. Humbert, H. Miller, Elevation and elevation change of Greenland and Antarctica derived from CryoSat-2. *The Cryosphere Discussions* **8**, 1673 (2014).
5. D. G. Vaughan *et al.*, in *Climate Change 2013: The Physical Science Basis. Contribution of Working Group I to the Fifth Assessment Report of the Intergovernmental Panel on Climate Change* T. F. Stocker *et al.*, Eds. (Cambridge University Press, Cambridge, 2013), pp. 317-382.
6. S. Levitus *et al.*, Global ocean heat content 1995-2008 in light of recently revealed instrumentation problems. *Geophysical Research Letters* **36**, L07608 (2009).
7. A. Abe-Ouchi *et al.*, Insolation-driven 100,000-year glacial cycles and hysteresis of ice-sheet volume. *Nature* **500**, 190 (2013).
8. V. Masson-Delmotte *et al.*, in *Climate Change 2013: The Physical Science Basis. Contribution of Working Group I to the Fifth Assessment Report of the Intergovernmental Panel on Climate Change,* T. F. Stocker *et al.*, Eds. (Cambridge University Press, Cambridge, 2013).

9. J. Ridley, J. M. Gregory, P. Huybrechts, J. Lowe, Thresholds for irreversible decline of the Greenland ice sheet. *Climate Dynamics* **35**, 1049 (2009).
10. J. Hansen, M. Sato, G. Russell, P. Kharecha, Climate sensitivity, sea level and atmospheric carbon dioxide. *Philosophical Transactions of the Royal Society* **371**, 1 (2013).
11. G. L. Foster, E. J. Rohling, Relationship between sea level and climate forcing by CO_2 on geological timescales. *Proceedings of the National Academy of Sciences*, (2013).
12. D. Pollard, R. M. DeConto, Modelling West Antarctic ice sheet growth and collapse through the past five million years. *Nature* **458**, 329 (2009).
13. J. X. Mitrovica, N. Gomez, J. Clark, The sea-level fingerprint of West Antarctic collapse. *Science* **323**, 753 (2009).
14. M. Pagani, Z. Liu, J. LaRiviere, A. C. Ravelo, High Earth-system climate sensitivity determined from Pliocene carbon dioxide concentrations. *Nature Geoscience* **3**, 27 (2010).
15. O. Seki, G. L. Foster, D. N. Schmidt, A. Mackensen, K. Kawamura, Alkenone and boron-based Pliocene pCO_2 records. *Earth and Planetary Science Letters* **292**, 201 (2010).
16. A. M. Haywood *et al.*, Large-scale features of Pliocene climate: results from the Pliocene Model Intercomparison Project. *Climate of the Past* **9**, 191 (2013).
17. H. J. Dowsett *et al.*, Sea Surface Temperature of the mid-Piacenzian Ocean: A Data-Model Comparison. *Scientific Reports* **3**, 1 (2013).
18. M. E. Raymo, J. X. Mitrovica, M. J. O'Leary, R. M. DeConto, P. J. Hearty, Departures from eustasy in Pliocene sea-level records. *Nature Geoscience* **4**, 328 (2011).
19. T. Naish, R. Powell, R. Levy, G. Wilson, R. Scherer, Obliquity-paced Pliocene West Antarctic ice sheet oscillations. *Nature* **458**, 322 (2009).
20. C. P. Cook *et al.*, Dynamic behaviour of the East Antarctic ice sheet during Pliocene warmth. *Nature Geoscience* **6**, 765 (2013).
21. M. O. Patterson *et al.*, Orbital forcing of the East Antarctic ice sheet during the Pliocene and Early Pleistocene. *Nature Geoscience* **7**, 841 (2014).
22. S. J. Koenig, R. M. DeConto, D. Pollard, Impact of reduced Arctic sea ice on Greenland ice sheet variability in a warmer than present climate. *Geophysical Research Letters* **41**, 3933 (2014).
23. H. Dowsett, T. M. Cronin, High eustatic sea level during the middle Pliocene: Evidence from the southeastern US Atlantic Coastal Plain. *Geology* **18**, 435 (1990).
24. K. Miller *et al.*, High tide of the warm Pliocene: Implications of global sea level for Antarctic deglaciation. *Geology* **40**, 407 (2012).
25. D. E. Krantz, A chronology of Pliocene sea-level fluctuations: The US Middle Atlantic coastal plain record. *Quaternary Science Reviews* **10**, 163 (1991).
26. T. R. Naish, G. S. Wilson, Constraints on the amplitude of Mid-Pliocene (3.6-2.4 Ma) eustatic sea-level fluctuations from the New Zealand shallow-marine sediment record. *Philosophical Transactions of the Royal Society* **367**, 169 (2009).
27. B. R. Wardlaw, T. M. Quinn, The record of Pliocene sea-level change at Enewetak Atoll. *Quaternary Science Reviews* **10**, 247 (1991).
28. D. B. Rowley *et al.*, Dynamic topography change of the eastern United States since 3 million years ago. *Science* **340**, 1560 (2013).
29. A. Rovere *et al.*, The Mid-Pliocene sea-level conundrum: Glacial isostasy, eustasy and dynamic topography. *Earth and Planetary Science Letters* **387**, 27 (2014).

30. G. S. Dwyer, M. A. Chandler, Mid-Pliocene sea level and continental ice volume based on coupled benthic Mg/Ca palaeotemperatures and oxygen isotope. *Royal Society of London Philosophical Transactions* **367**, 157 (2009).
31. S. Sosdian, Y. Rosenthal, Deep-sea temperature and ice volume changes across the Pliocene-Pleistocene climate transitions. *Science* **325**, 306 (2009).
32. J. Yu, W. S. Broecker, Comment on "Deep-Sea Temperature and Ice Volume Changes Across the Pliocene-Pleistocene Climate Transitions". *Science* **328**, 1480 (2010).
33. R. Kozdon *et al.*, In situ $\delta^{18}O$ and Mg/Ca analyses of diagenetic and planktic foraminiferal calcite preserved in deep-sea record of the Paleocene-Eocene thermal maximum. *Paleoceanography* **28**, 517 (2013).
34. C. L. O'Brien *et al.*, High sea surface temperatures in tropical warm pools during the Pliocene. *Nature Geoscience* **7**, 606 (2014).
35. L. E. Lisiecki, M. E. Raymo, A Pliocene-Pleistocene stack of 57 globally distributed benthic $\delta^{18}O$ records. *Paleoceanography* **20**, PA1003 (2005).
36. N. Lang, E. W. Wolff, Interglacial and glacial variability from the last 800 ka in marine, ice and terrestrial archives. *Climate of the Past* **7**, 361 (2011).
37. Q. Z. Yin, A. Berger, Insolation and CO_2 contribution to the interglacial climate before and after the Mid-Brunhes Event. *Nature Geoscience* **3**, 243 (2010).
38. V. Masson-Delmotte *et al.*, EPICA Dome C record of glacial and interglacial intensities. *Quaternary Science Reviews* **29**, 113 (2010).
39. D. Lüthi *et al.*, High-resolution carbon dioxide concentration record 650,000–800,000 years before present. *Nature* **453**, 379 (2008).
40. T. M. Cronin *et al.*, A 600-ka Arctic sea-ice record from Mendeleev Ridge based on ostracodes. *Quaternary Science Reviews* **79**, 157 (2013).
41. M. Melles *et al.*, 2.8 Million Years of Arctic Climate Change from Lake El'gygytgyn, NE Russia. *Science* **337**, 315 (2012).
42. J. Jouzel *et al.*, Orbital and Millennial Antarctic Climate Variability over the Past 800,000 Years. *Science* **317**, 793 (2007).
43. A. J. Coletti, R. M. DeConto, J. Brigham-Grette, M. Melles, A GCM comparison of Plio–Pleistocene interglacial–glacial periods in relation to Lake El'gygytgyn, NE Arctic Russia. *Climate of the Past Discussions* **10**, 3127 (2014).
44. A. de Vernal, C. Hillaire-Marcel, Natural Variability of Greenland Climate, Vegetation, and Ice Volume During the Past Million Years. *Science* **320**, 1622 (2008).
45. E. Willerslev *et al.*, Ancient Biomolecules from Deep Ice Cores Reveal a Forested Southern Greenland. *Science* **317**, 111 (2007).
46. A. V. Reyes *et al.*, South Greenland ice-sheet collapse during Marine Isotope Stage 11. *Nature* **510**, 525 (2014).
47. H. A. Bauch, Interglacial climates and the Atlantic meridional overturning circulation: is there an Arctic controversy? *Quaternary Science Reviews* **63**, 1 (2013).
48. R. McKay *et al.*, Pleistocene variability of Antarctic Ice Sheet extent in the Ross Embayment. *Quaternary Science Reviews* **34**, 93 (2012).
49. C. V. Murray-Wallace, Pleistocene coastal stratigraphy, sea-level highstands and neotectonism of the southern Australian passive continental margin?a review. *Journal of Quaternary Science* **17**, 469 (2002).

50. P. J. Hearty, P. Kindler, H. Cheng, R. L. Edwards, A +20 m middle Pleistocene sea-level highstand (Bermuda and the Bahamas) due to partial collapse of Antarctic ice. *Geology* **27**, 375 (1999).
51. M. E. Raymo, J. X. Mitrovica, Collapse of polar ice sheets during the stage 11 interglacial. *Nature* **483**, 453 (2012).
52. D. L. Roberts, P. Karkanas, Z. Jacobs, C. W. Marean, R. G. Roberts, Melting ice sheets 400,000 yr ago raised sea level by 13m: Past analogue for future trends. *Earth and Planetary Science Letters* **357-358**, 226 (2012).
53. F. Chen *et al.*, Refining Estimates of Polar Ice Volumes During the MIS11 Interglacial Using Sea Level Records from South Africa. *Journal of Climate* **27**, 8740 (2014).
54. H. Elderfield *et al.*, Evolution of Ocean Temperature and Ice Volume Through the Mid-Pleistocene Climate Transition. *Science* **337**, 704 (2012).
55. E. J. Rohling *et al.*, Antarctic temperature and global sea level closely coupled over the past five glacial cycles. *Nature Geoscience* **2**, 500 (2009).
56. M. Siddall *et al.*, Sea-level fluctuations during the last glacial cycle. *Nature* **423**, 853 (2003).
57. C. H. Stirling, T. M. Esat, K. Lambeck, M. T. McCulloch, Timing and duration of the Last Interglacial: evidence for a restricted interval of widespread coral reef growth. *Earth and Planetary Science Letters* **160**, 745 (1998).
58. B. Otto-Bliesner *et al.*, How warm was the last interglacial? New model–data comparisons. *Philosophical Transactions of the Royal Society A* **371**, 20130097. (2013).
59. CAPE Last Interglacial Project Members, Last Interglacial Arctic warmth confirms polar amplification of climate change. *Quaternary Science Reviews* **25**, 1383 (2006).
60. D. Dahl-Jensen *et al.*, Eemian interglacial reconstructed from a Greenland folded ice core. *Nature* **493**, 489 (2013).
61. A. Dutton, K. Lambeck, Ice volume and sea level during the Last Interglacial. *Science* **337**, 216 (2012).
62. R. E. Kopp, F. J. Simons, J. X. Mitrovica, A. C. Maloof, M. Oppenheimer, Probabilistic assessment of sea level during the last interglacial stage. *Nature* **462**, 863 (2009).
63. A. Dutton, J. M. Webster, D. Zwartz, K. Lambeck, B. Wohlfarth, Tropical tales of polar ice: Evidence of last interglacial polar ice sheet retreat recorded by fossil reefs of the granitic Seychelles islands. *Quaternary Science Reviews* **107**, 182 (2015).
64. M. J. O'Leary *et al.*, Ice sheet collapse following a prolonged period of stable sea level during the last interglacial. *Nature Geoscience* **6**, 796 (2013).
65. K. M. Grant *et al.*, Rapid coupling between ice volume and polar temperature over the past 150,000 years. *Nature* **491**, 744 (2012).
66. K. Lambeck *et al.*, Sea level and shoreline reconstructions for the Red Sea: isostatic and tectonic considerations and implications for hominin migration out of Africa. *Quaternary Science Reviews* **30**, 3542 (2011).
67. E. J. Colville *et al.*, Sr-Nd-Pb isotope evidence for ice-sheet presence on southern Greenland during the Last Interglacial. *Science* **333**, 620 (2011).
68. N. P. McKay, J. T. Overpeck, B. L. Otto-Bliesner, The role of ocean thermal expansion in Last Interglacial sea level rise. *Geophysical Research Letters* **38**, L14605 (2011).
69. R. P. Scherer *et al.*, Pleistocene collapse of the West Antarctic Ice Sheet. *Science* **281**, 82 (1998).

70. C. D. Gallup, R. L. Edwards, R. G. Johnson, The timing of high sea levels over the past 200,000 years. *Science* **263**, 796 (1994).
71. P. Blanchon, A. Eisenhauer, J. Fietzke, V. Liebetrau, Rapid sea-level rise and reef back-stepping at the close of the last interglacial highstand. *Nature* **458**, 881 (2009).
72. J. H. Chen, H. A. Curran, B. White, G. J. Wasserburg, Precise chronology of the last interglacial period: ^{234}U-^{230}Th data from fossil coral reefs in the Bahamas. *Geological Society of America Bulletin* **103**, 82 (1991).
73. P. J. Hearty, J. T. Hollin, A. C. Neumann, M. J. O'Leary, M. T. McCulloch, Global sea-level fluctuations during the Last Interglaciation (MIS 5e). *Quaternary Science Reviews* **26**, 2090 (2007).
74. W. G. Thompson, H. A. Curran, M. A. Wilson, B. White, Sea-level and ice-sheet instability during the Last Interglacial: new Bahamas evidence. *Nature Geoscience* **4**, 684 (2011).
75. E. J. Rohling *et al.*, High rates of sea-level rise during the last interglacial period. *Nature Geoscience* **1**, 38 (2008).
76. J.-C. Plazait, J.-L. Reyss, A. Choukri, C. Cazala, Diagenetic rejuvenation of raised coral reefs and precision of dating. The contribution of the Red Sea reefs to the question of reliability of the Uranium-series datings of middle to late Pleistocene key reef-terraces of the world. *Carnets de Géologie* **CG2008**, 1 (2008).
77. R. E. Kopp, F. J. Simons, J. X. Mitrovica, A. C. Maloof, M. Oppenheimer, A probabilistic assessment of sea level variations within the last interglacial stage. *Geophysical Journal International* **193**, 711 (2013).
78. S. A. Marcott, J. D. Shakun, P. U. Clark, A. C. Mix, A Reconstruction of Regional and Global Temperature for the Past 11,300 Years. *Science* **339**, 1198 (2013).
79. D. L. Hartmann *et al.*, in *Climate Change 2013: The Physical Science Basis. Contribution of Working Group I to the Fifth Assessment Report of the Intergovernmental Panel on Climate Change,* T. F. Stocker *et al.*, Eds. (Cambridge University Press, Cambridge, UK, 2013), pp. 159-254.
80. Z. Liu *et al.*, The Holocene temperature conundrum. *Proceedings of the National Academy of Sciences* **111**, E3501 (2014).
81. A. C. Kemp *et al.*, Climate related sea-level variations over the past two millennia. *Proceedings of the National Academy of Sciences* **108**, 11017 (2011).
82. K. Lambeck, H. Rouby, A. Purcell, Y. Sun, M. Sambridge, Sea level and global ice volumes from the Last Glacial Maximum to the Holocene. *Proceedings of the National Academy of Sciences* **111**, 15296 (2014).
83. K. Fleming *et al.*, Refining the eustatic sea-level curve since the Last Glacial Maximum using far and intermediate-field sites. *Earth and Planetary Science Letters* **163**, 327 (1998).
84. M. J. Bentley, The Antarctic palaeo record and its role in improving predictions of future Antarctic Ice Sheet change. *Journal of Quaternary Science* **25**, 5 (2010).
85. J. O. Stone *et al.*, Holocene Deglaciation of Marie Byrd Land, West Antarctica. *Science* **299**, 99 (2003).
86. A. J. Long, S. A. Woodroffe, D. H. Roberts, S. Dawson, Isolation basins, sea-level changes and the Holocene history of the Greenland Ice Sheet. *Quaternary Science Reviews* **30**, 3748 (2011).

87. A. E. Carlson *et al.*, Earliest Holocene south Greenland ice sheet retreat within its late Holocene extent. *Geophysical Research Letters* **41**, 5514 (2014).
88. B. S. Lecavalier, G. A. Milne, M. Simpson, L. Wake, A model of Greenland ice sheet deglaciation constrained by observations of relative sea level and ice extent. *Quaternary Science Reviews* **102**, 54 (2014).
89. J. A. Clark, W. E. Farrell, W. R. Peltier, Global changes in postglacial sea level: A numerical calculation. *Quaternary Research* **9**, 265 (1978).
90. J. X. Mitrovica, G. A. Milne, On the origin of late Holocene sea-level highstands within equatorial ocean basins. *Quaternary Science Reviews* **21**, 2179 (2002).
91. J. S. Compton, Holocene sea-level fluctuations inferred from the evolution of depositional environments of the southern Langebaan Lagoon salt marsh, South Africa. *The Holocene* **11**, 395 (2001).
92. K. Rostami, W. R. Peltier, A. Mangini, Quaternary marine terraces, sea-level changes and uplift history of Patagonia, Argentina: comparisons with predictions of the ICE-4G (VM2) model of the global process of glacial isostatic adjustment. *Quaternary Science Reviews* **19**, 1495 (2000).
93. A. C. Kemp *et al.*, Climate related sea level variations over the past two millennia. Proceedings of the National Academy of Sciences. *Proceedings of the National Academy of Sciences* **108**, 11017 (2011).
94. A. Long *et al.*, Contrasting records of sea-level change in the eastern and western North Atlantic during the last 300 years. *Earth and Planetary Science Letters* **388**, 110 (2014).
95. R. E. Kopp *et al.*, The impact of Greenland melt on local sea levels: a partially coupled analysis of dynamic and static equilibrium effects in idealized water-hosing experiments. *Climatic Change* **103**, 619 (2010).
96. J. S. Johnson *et al.*, Rapid Thinning of Pine Island Glacier in the Early Holocene. *Science* **343**, 999 (2014).
97. C. H. Stirling, M. B. Andersen, Uranium-series dating of fossil coral reefs: Extending the sea-level record beyond the last glacial cycle. *Earth and Planetary Science Letters* **284**, 269 (2009).
98. J. Austermann, J. X. Mitrovica, K. Latychev, G. A. Milne, Barbados based estimate of ice volume at Last Glacial Maximum effected by subducted plate. *Nature Geoscience* **6**, 553 (2013).
99. G. Camoin, J. M. Webster, Coral reef response to Quaternary sea-level and environmental changes: State of the science. *Sedimentology* **62**, 401 (2015).
100. P. Deschamps *et al.*, Ice-sheet collapse and sea-level rise at the Bolling warming 14,600 years ago. *Nature* **483**, 559 (2012).
101. L. J. Gregoire, A. J. Payne, P. J. Valdes, Deglacial rapid sea level rises caused by ice-sheet saddle collapses. *Nature* **487**, (2012).
102. S. A. Marcott *et al.*, Ice-shelf collapse from subsurface warming as a trigger for Heinrich events. *Proceedings of the National Academy of Sciences* **108**, 13415 (2011).
103. C. Hay *et al.*, The sea-level fingerprints of ice-sheet collapse during interglacial periods. *Quaternary Science Reviews* **87**, 60 (2014).
104. R. M. DeConto, D. Pollard, D. Kowalewski, Modeling Antarctic ice sheet and climate variations during Marine Isotope Stage 31. *Global and Planetary Change* **88-89**, 45 (2012).

105. M. Mengel, A. Levermann, Ice plug prevents irreversible discharge from East Antarctica. *Nature Climate Change* **4**, 451 (2014).
106. P. U. Clark, J. X. Mitrovica, G. A. Milne, M. E. Tamisiea, Sea-level fingerprinting as a direct test for the source of global meltwater pulse IA. *Science* **295**, 2438 (2002).
107. J. C. Zachos, M. Pagani, L. Sloan, E. Thomas, K. Billups, Trends, rhythms, and aberrations in global climate 65 Ma to present. *Science* **292**, 686 (2001).
108. E. J. Rohling *et al.*, Sea-level and deep-sea-temperature variability over the past 5.3 million years. *Nature* **508**, 477 (2014).
109. W. E. Farrell, J. A. Clark, On postglacial sea-level. *Geophysical Journal of the Royal Astronomical Society* **46**, 647 (1976).
110. K. Lambeck, C. Smither, P. Johnston, Sea-level change, glacial rebound and mantle viscosity for northern Europe. *Geophysical Journal International* **134**, 102 (1998).
111. L. Tarasov, A. S. Dyke, R. M. Neal, W. R. Peltier, A data-calibrated distribution of deglacial chronologies for the North American ice complex from glaciological modeling. *Earth and Planetary Science Letters* **315-316**, 30 (2012).
112. A. M. Tushingham, W. R. Peltier, Ice-3G: a new global model of late Pleistocene deglaciation based upon geophysical predictions of post-glacial relative sea-level change. *Journal of Geophysical Research* **96**, 4497 (1991).
113. P. Wu, W. Van der Wal, Postglacial sea-levels on a spherical, self-gravitating viscoelastic earth: effects of lateral viscosity variations in the upper mantle on the inference of viscosity contrasts in the lower mantle. *Earth and Planetary Science Letters* **211**, 57 (2003).
114. C. P. Conrad, B. H. Hager, Spatial variations in the rate of sea level rise caused by present-day melting of glaciers and ice sheets. *Geophysical Research Letters* **24**, 1503 (1997).
115. J. X. Mitrovica, M. E. Tamisiea, J. L. Davis, G. A. Milne, Recent mass balance of polar ice sheets inferred from patterns of global sea-level change. *Nature* **409**, 1026 (2001).
116. J. A. Clark, C. S. Lingle, Future sea-level changes due to West Antarctic ice sheet fluctuations. *Nature* **269**, 206 (1977).
117. M. Gurnis, Rapid continental subsidence following the initiation and evolution of subduction. *Science* **255**, 1556 (1992).
118. D. P. McKenzie, Surface deformation, gravity anomalies and convection. *Geophysical Journal of the Royal Astronomical Society* **48**, 211 (1977).
119. J. X. Mitrovica, C. Beaumont, G. T. Jarvis, Tilting of continental interiors by the dynamical effects of subduction. *Tectonics* **8**, 1079 (1989).
120. C. P. Conrad, L. Husson, Influence of dynamic topography on sea level and its rate of change. *Lithosphere* **1**, 110 (2009).
121. R. Moucha *et al.*, Dynamic topography and long-term sea-level variations: There is no such thing as a stable continental platform. *Earth and Planetary Science Letters* **271**, 101 (2008).
122. R. D. Muller, M. Sdrolias, C. Gaina, B. Steinberger, C. Heine, Long-Term Sea-Level Fluctuations Driven by Ocean Basin Dynamics. *Science* **319**, 1357 (2008).
123. E. A. Neil, G. A. Housemann, Rayleigh-Taylor instability of the upper mantle and its role in intraplate orogeny. *Geophysical Journal International* **138**, 89 (1999).

124. R. N. Pysklywec, C. Beaumont, Intraplate tectonics: feedback between radioactive thermal weakening and crustal deformation driven by mantle lithosphere instabilitie. *Earth and Planetary Science Letters* **221**, 275 (2004).
125. S. Zhong, A. McNamara, E. Tan, L. Moresi, M. Gurnis, A benchmark study on mantle convection in a 3-D spherical shell using CitcomS. *Geochemistry, Geophysics, Geosystems* **9**, Q10017 (2008).
126. W. R. Peltier, Global glacial isostasy and the surface of the ice-age Earth: The ICE-5G (VM2) Model and GRACE. *Annual Review of Earth and Planetary Sciences* **32**, 111 (2004).

Acknowledgments: This manuscript was developed based on collaborations and discussions that have stemmed from the PALSEA and PALSEA2 working group, presently funded by PAGES and INQUA. We thank four anonymous reviewers for comments that helped to improve the manuscript, A. Kemp for assistance with one of the figures, and A. Rovere, B. Honisch for helpful comments. Funding was provided by NSF awards #1155495 to AD, #1202632 to MER, #1343573 to AEC, #0958417 and #1043517 to PUC, OCE1458904 to BPH, and NERC Grant NE/I008675/1 to AJL.

Text Box 1. Methods of Reconstructing Past Sea Level and Ice Volume

Sea-level reconstructions: In our analysis of sea-level reconstructions, we consider two categories separately: those that are derived from $\delta^{18}O$ of marine carbonates (hereafter termed $\delta^{18}O$-proxy records) and those based on direct observational evidence of sea level or shoreline elevation (hereafter termed coastal records).

There are three types of $\delta^{18}O$-proxy records used to estimate former GMSL: (i) benthic $\delta^{18}O$, which comprises a combined signal of temperature and global ice volume (*107*), (ii) benthic or planktic $\delta^{18}O$ in foraminifera or ostracods, paired with a proxy that can independently constrain the temperature component embedded in this signal (*31, 54*), (iii) planktic $\delta^{18}O$ from evaporative marginal seas which is transformed into a RSL signal using hydraulic models that constrain the salinity of surface waters as a function of sea level (e.g., *56*). Each of these geochemical approaches entails certain assumptions and uncertainties, and we note that in the case of isolated basins such as the Red Sea or Mediterranean (*56, 108*) additional corrections and assumptions about regional hydrology, relative humidity, and tectonic stability and isostatic response of the sill depth must also be made in addition to assumptions about how sea surface temperature changed.

Coastal records of former sea level reflect RSL rather than GMSL. Each RSL record has uncertainties in its age and elevation that are primarily a function of the dating technique(s) and the nature of the geologic archive, respectively. Coastal records include geomorphological features, shallow-water corals, and salt-marsh records that directly track the elevation of RSL through time. To associate changes in RSL to GMSL, one must quantify and correct for geophysical processes (described below) that may contribute significantly to RSL at the site (Fig. 1). Glacial isostatic adjustment (GIA) is arguably the most important of these processes as it can influence the present-day elevation of sea-level indicators from any time period in the past. Additional processes operate on more specific space and time scales and thus only become important at those particular scales of analysis (Fig. 1). For example, inter-annual to multi-decadal ocean-atmosphere interactions such as the North Atlantic Oscillation or the Pacific Decadal Oscillation can cause RSL fluctuations of up to several decimeters. Such processes are important when interpreting highly resolved reconstructions such as those from instrumental records or from late-Holocene geologic archives. On the other hand, dynamic topography resulting from flow in the Earth's mantle can dominate the RSL signal over timescales of millions of years and produce high-amplitude (meter- to multi-meter scale) variability.

Glacial isostatic adjustment (GIA): The water mass transfer between the ice sheets and oceans during glacial-interglacial cycles causes changes in the Earth's shape, gravity field, and rotation that create a distinct spatial pattern to RSL across the globe (*109*) (Fig. 2). These GIA processes dominate the spatial variability in sea-level change over millennial time scales during the Quaternary and are also a significant (several mm yr^{-1}) background component to recent (historical) sea-level change (Fig. 2). GIA is also an important contributor to RSL for older time periods due, in part, to the fact that the solid Earth is continuing to isostatically adjust to the most recent deglaciation (*18*).

GIA models are primarily driven by an *a priori* ice model that defines the volume and geographic extent of grounded ice through time, which is then used to solve for the elevation of the shorelines and the changes in the height of the ocean floor and sea surface—the latter being affected by changes in gravity. The ice model is constrained by field evidence on the timing, thickness, and geographic extent of ice as well as by constraints from observations of the elevation of RSL through time from sites close to ("near-field") and far from ("far-field") the former ice sheets (e.g., *110, 111, 112*). The other key component of GIA models is an Earth model that is defined by layer thicknesses, viscosity, elasticity and density of the Earth's interior, which in turn dictate the way in which the Earth's surface responds and deforms to the assumed ice-load history. Typically global GIA models are run using a single, laterally homogeneous Earth model. Regional studies are often used to explore variations in the Earth model that provide a better fit to data in that area. More recently, 3-D GIA models have been applied to examine the influence of lateral Earth structure on RSL changes (e.g., *98, 113*).

GIA models typically simulate global patterns in RSL change due to ice melting over relatively short timescales (10s to 100s of years). In this case, the solid Earth response is dominantly elastic and so accurately defining the viscosity structure, a primary source of GIA model uncertainty, becomes less important. Since the elastic properties of the Earth are relatively well defined from seismic investigations, the computed RSL response can be accurately interpreted in terms of melt-source location. In other words, the spatial pattern of RSL change can be used to 'fingerprint' melt sources, hence the use of the term 'sea-level fingerprinting' for this application. This technique has been applied to rapid melting events in the geological record (*103, 106*), 20th century sea-level change (*114, 115*) and regional projections of future change (*13, 116*).

Dynamic topography: Lateral motion of the Earth's tectonic plates (lithosphere) is due to buoyancy driven viscous flow of the mantle that can also lead to vertical motion of the Earth's surface through plate convergence and consequent lithospheric deformation (e.g., orogenesis). However, the same viscous flow of the mantle also results in normal stresses at the solid Earth-ocean/atmosphere interface, which can produce a vertical deflection of this interface of up to a few km in amplitude (*117-119*). This component of the Earth's topography is associated with convectively supported vertical stresses and is termed "dynamic topography." (Note that the same term is also used in oceanography to described undulations in the sea surface associated with flow within the ocean.) As the distribution of density structure within the mantle evolves with time, so does the surface dynamic topography, resulting in significant changes in both local RSL and GMSL on timescales of 1-100 Ma (*120-122*). Vertical motion associated with dynamic topography also results in lateral stresses that can cause significant crustal deformation and thus additional vertical motion at the Earth's surface (*123, 124*). This additional component of vertical motion has yet to be considered in calculations of dynamic topography applied to sea-level studies.

Numerical models of mantle flow (e.g., *125*) are used to compute dynamic topography and predict how it evolves with time. The two primary inputs to these models are a 3-D density anomaly field to drive the simulation of material flow in the mantle as well as a radial viscosity profile that governs the rate of flow at a given depth in the mantle. The 3-D density field is estimated from seismic models of the Earth's internal velocity structure, which reflects both thermal and chemical variations within the mantle. The scaling from seismic velocity structure to density structure is not straightforward as it involves assumptions regarding the cause of seismic velocity variations (thermal, chemical or both; *120, 121*). It is this uncertainty in defining the input density structure, as well as our relatively poor knowledge of the Earth's viscosity structure, that limits the accuracy of modeled sea-level changes due to variations in dynamic topography.

Ice sheets: Ice-sheet reconstructions are informed primarily by direct observations of ice-margin and thickness data and nearby marine sediment and RSL records. Ice-rafted debris (IRD) and sediment provenance from geochemical analyses in marine cores are particularly useful for extending ice-sheet reconstructions farther back in time beyond the last deglaciation (i.e., >21 ka).

FIGURES

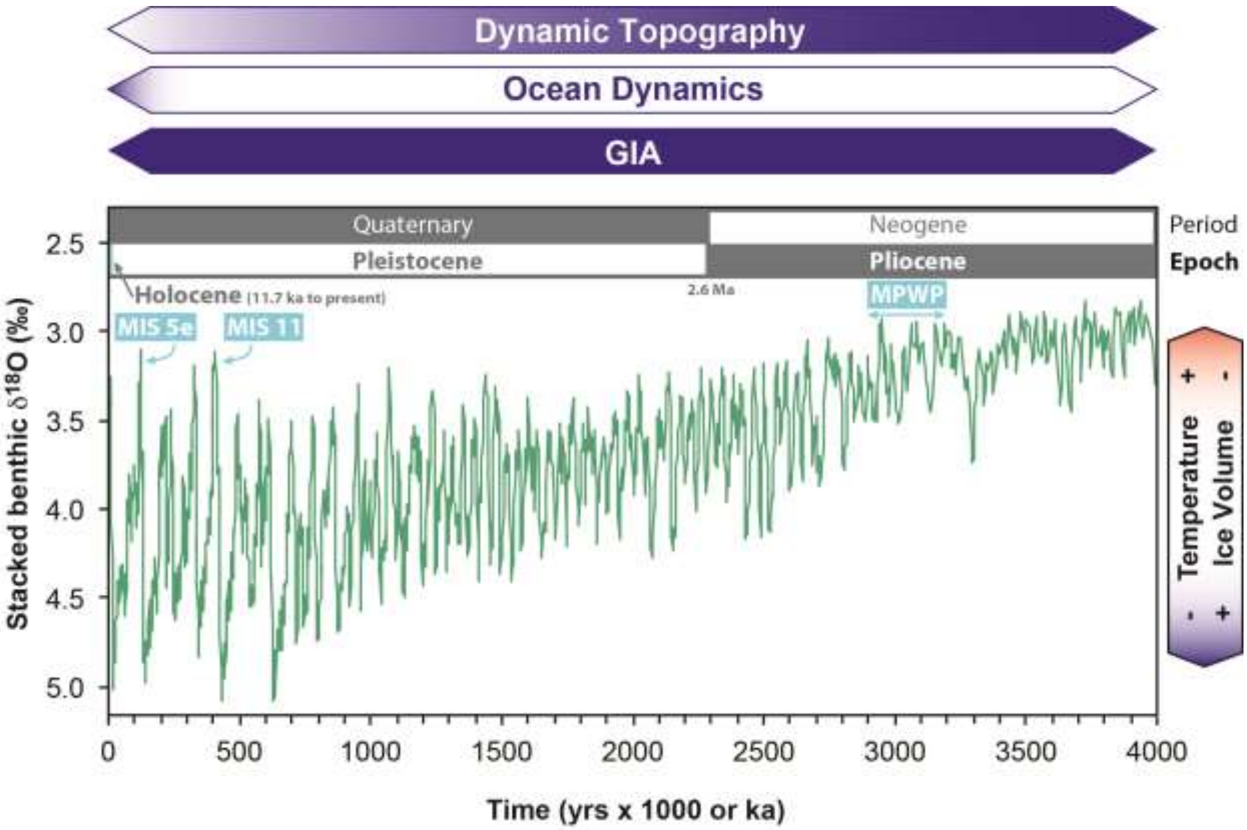

Figure 1. Stacked benthic $\delta^{18}O$ with time periods discussed in text. Benthic $\delta^{18}O$ (green curve--LR04; ref. *32*) provides a combined signal of ice volume and temperature deep into the geologic past (*107*). Physical processes that contribute to RSL signals (blue bars): length of blue bars indicates timespan over which the process is active; shading denotes time interval where the process can have the most significant influence on RSL reconstructions. For example, the rates of dynamic topography are slow enough that it generally is only a significant factor for reconstructing older paleoshorelines, as denoted by shading. GIA can dominate spatial variability in RSL across all of these timescales.

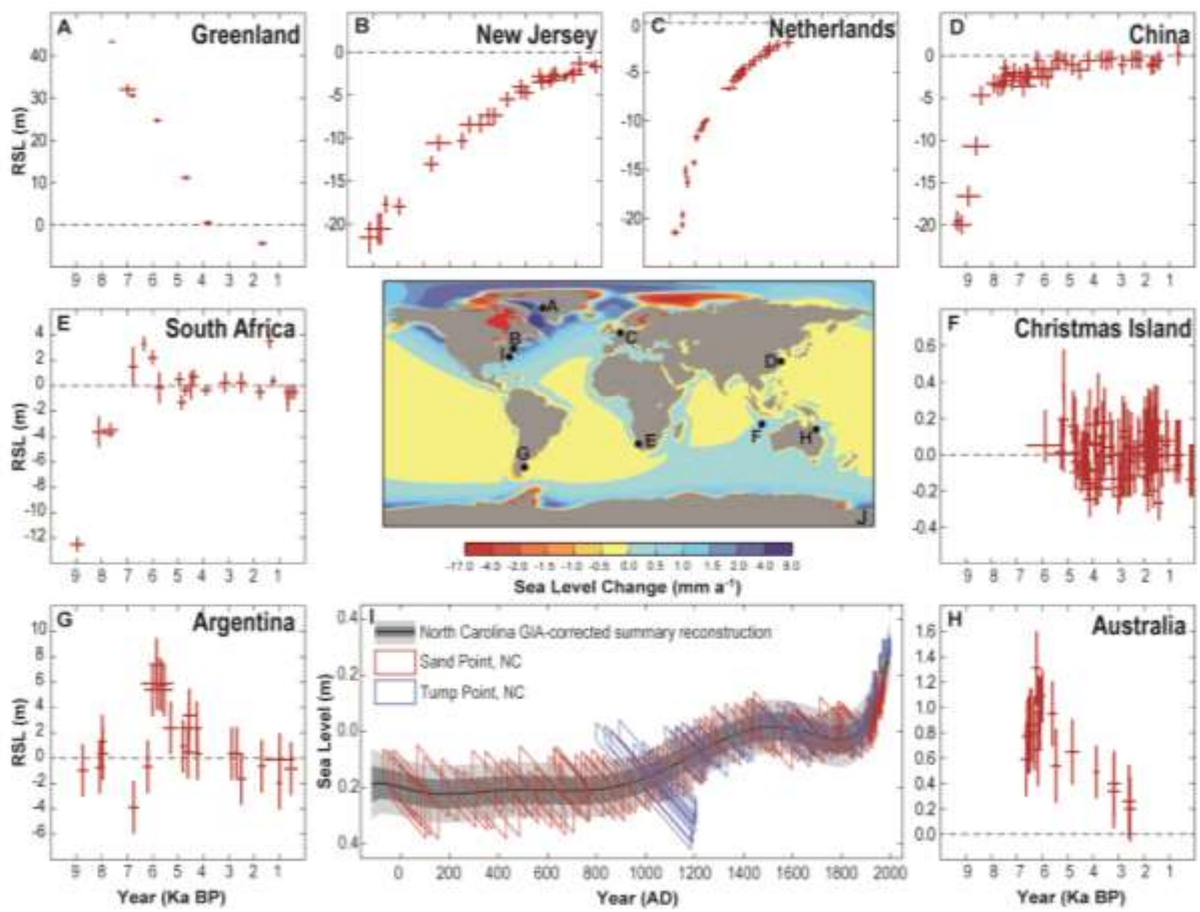

Figure 2. Selected Holocene relative sea-level (RSL) reconstructions. Elevations and interpretation of sea-level index points (including errors) have not been amended from the original publication. Radiocarbon ages were converted to calibrated dates where necessary, shown as calibrated years before present x 1000 (kyr BP). (A-I) Site locations and data sources are listed in Table S1. (I) GIA-adjusted sea level at North Carolina relative to a pre-Industrial average for 1400-1800 C.E. Center panel (J) shows rates of present sea-level change due to GIA, based on ICE-5G (*126*) and the VM2 Earth model with a 90-km thick lithosphere.

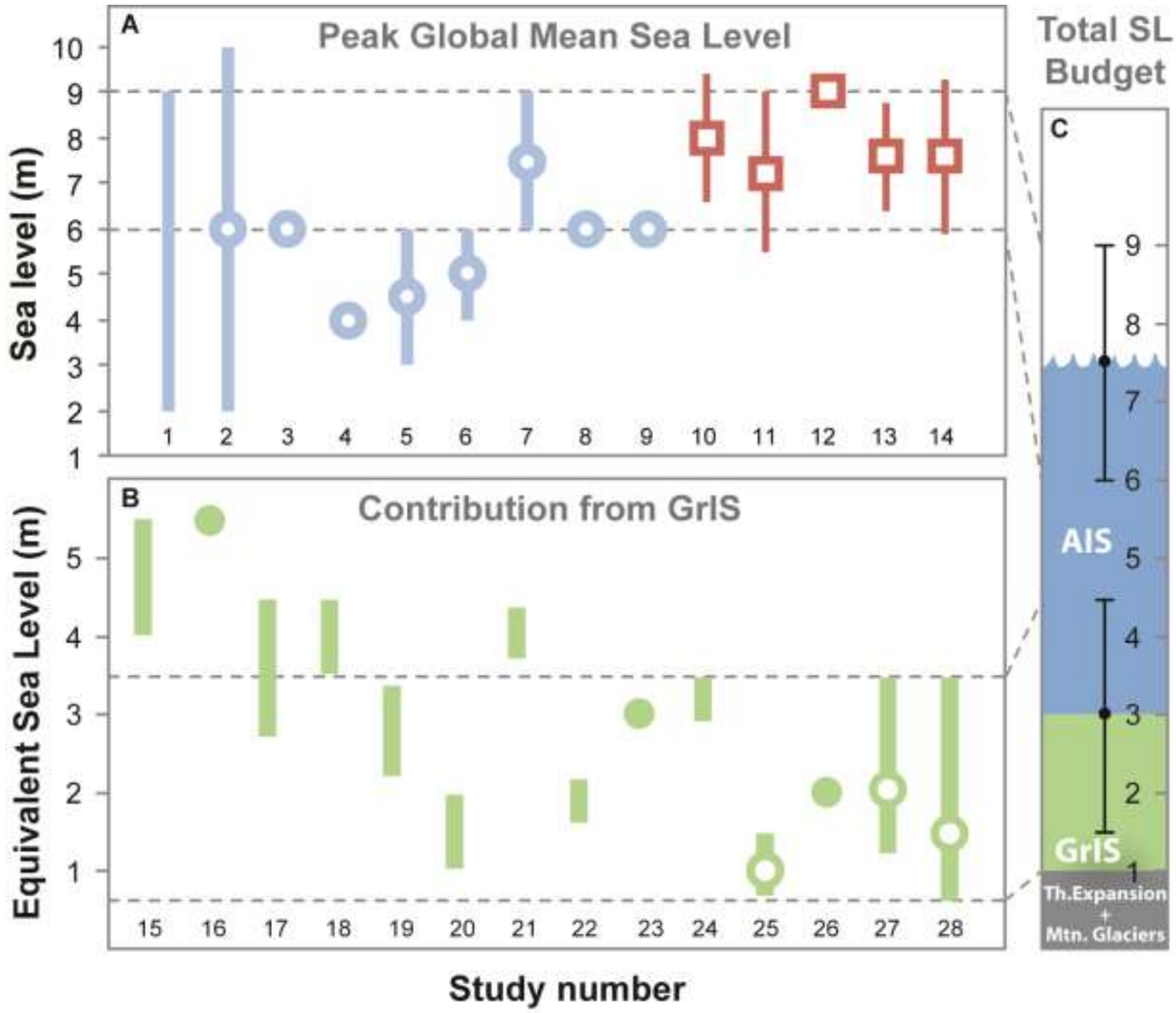

Figure 3. Compilation of MIS 5e reconstructions for peak GMSL, GrIS contribution, and best estimate of the total sea level budget. Estimates of (A) peak MIS 5e GMSL and (B) meltwater contribution from the GrIS shown in chronological order of time of publication from left to right. Ranges indicated by vertical bars; point estimates and best-estimates within ranges shown as circles. GIA-corrected records are shown in red squares. Horizontal dashed lines denote range of agreement between recent studies. (C) Total sea level budget of MIS 5e, shown with estimated uncertainty for each component. One meter is attributed to thermal expansion and loss of mountain glaciers (gray shading). As the

estimate of GrIS (green shading) has decreased, the overall peak SL estimate has grown, leading to increased confidence of a more substantial contribution from the AIS (blue shading). Data sources listed in Table S2.

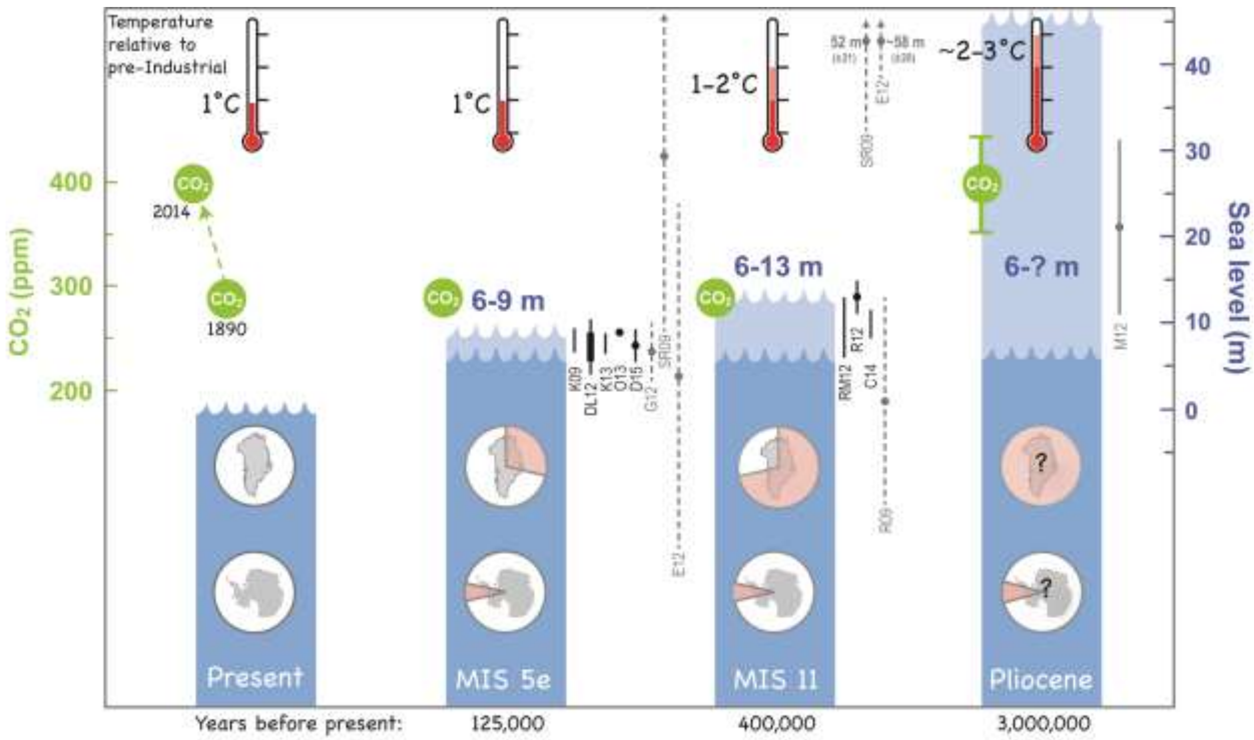

Figure 4. Peak global mean temperature, atmospheric CO_2, maximum GMSL, and source(s) of meltwater. Light blue shading indicates uncertainty of sea level maximum. Black vertical lines represent GMSL reconstructions from combined field observations and GIA modeling; gray dashed lines are $\delta^{18}O$-based reconstructions. Red pie charts over Greenland and Antarctica denote fraction (not location) of ice retreat. Although the peaks in temperature, CO_2, and sea level within each time period may not be synchronous and ice sheets are sensitive to factors not depicted here, note that significantly higher sea levels were attained during MIS 5e and 11 when atmospheric CO_2 forcing was significantly lower than present. See Tables S3-S4 for data and sources.

Supplementary Materials:

www.sciencemag.org
Figure S1
Tables S1 – S5
References (127-171)

Supplementary Materials for

Sea-level rise due to polar ice-sheet mass loss during past warm periods

A. Dutton, A. E. Carlson, A. J. Long, G. A. Milne, P. U. Clark, R. DeConto,
B. P. Horton, S. Rahmstorf, M. E. Raymo

correspondence to: adutton@ufl.edu

This PDF file includes:

Figure S1
Tables S1 to S5

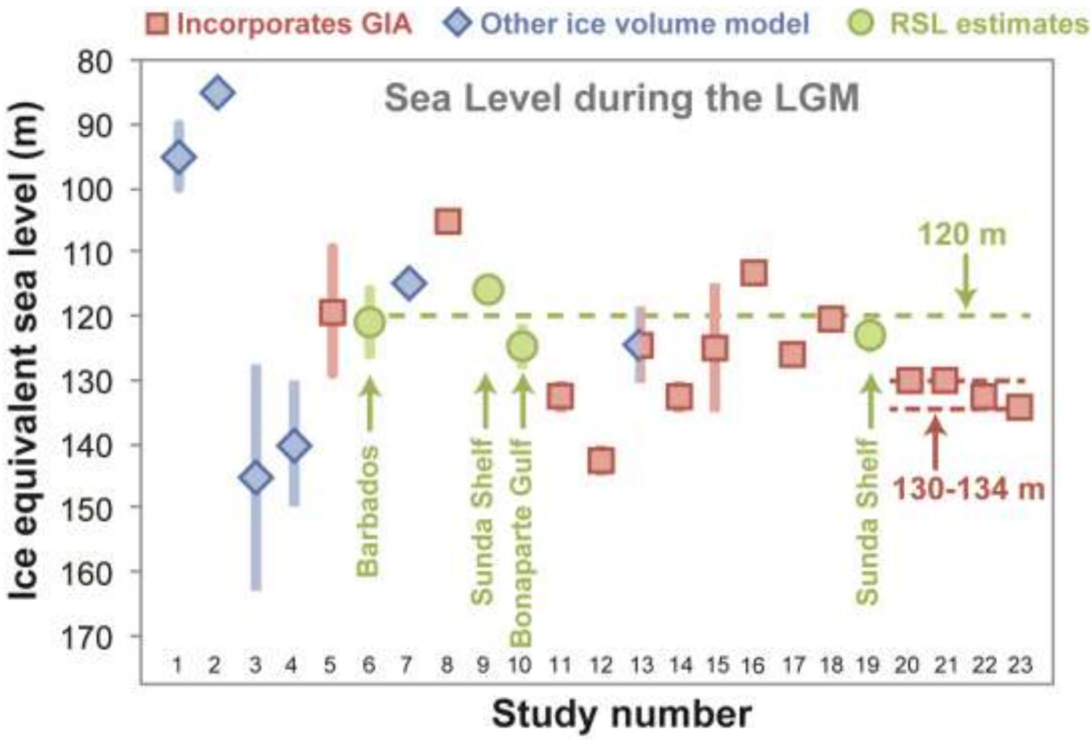

Figure S1.

Compilation of estimates of ice volume during the LGM (MIS 2) shown in chronological order of publication from left to right. Models of LGM ice volume draw upon the same observational datasets, hence the variability in GIA-based LGM ice volume estimates over time reflect the evolution of the modeling as well as differing interpretations of the observational data. Data sources listed in Table S5. Note that site-specific RSL positions of the LGM cluster near 120 m below present sea level where as many recent GMSL estimates from GIA models cluster in the range of 130-134 m.

Table S1.

Data sources for Holocene sea level reconstructions in Figure 2.

Figure Panel	Location	Study	Year	Source
A	Disko Bugt, Greenland	Long et al.	2006	(*127*)
B	New Jersey, USA	Horton et al.	2013	(*128*)
C	The Netherlands	Hijma & Cohen	2010	(*129*)
D	Yangtze Delta, China	Zong	2004	(*130*)
E	SW South Africa	Compton	2001	(*91*)
F	Christmas Island	Woodroffe et al.	2012	(*131*)
G	Patagonia, Argentina	Rostami et al.	2000	(*92*)
H	Orpheus Island, Australia	Lambeck	2002	(*132*)
I	North Carolina, USA	Kemp et al.	2011	(*81*)

Table S2.

Data sources for MIS 5e peak sea level (1-14) and for meters of equivalent sea level contribution from the Greenland Ice Sheet (15-28) shown in Figure 3.

Figure Source #	**Study**	**Year**	**Bibliography number**
1	Veeh	1966	(*133*)
2	Chappell and Shackleton	1986	(*134*)
3	Chen et al.	1991	(*72*)
4	Stirling et al.	1998	(*57*)
5	Muhs et al.	2002a	(*135*)
6	Muhs et al.	2002b	(*136*)
7	Hearty et al.	2007	(*73*)
8	Blanchon et al.	2009	(*71*)
9	Thompson et al.	2011	(*74*)
10	Kopp et al.	2009	(*62*)
11	Dutton and Lambeck	2012	(*61*)
12	O'Leary et al.	2013	(*64*)
13	Kopp et al.	2013	(*77*)
14	Dutton et al.	2015	(*63*)
15	Cuffey and Marshall	2000	(*137*)
16	Huybrechts	2002	(*138*)
17	Tarasov and Peltier	2003	(*139*)
18	L'homme et al.	2005	(*140*)
19	Otto-Bleisner et al.	2006	(*141*)
20	Oerlemans et al.	2006	(*142*)
21	Robinson et al.	2011	(*143*)
22	Colville et al.	2011	(*67*)
23	Fyke et al.	2011	(*144*)
24	Born and Nisancioglu	2012	(*145*)
25	Quiquet et al.	2013	(*146*)
26	Dahl-Jensen et al.	2013	(*60*)
27	Helsen et al.	2013	(*147*)
28	Stone et al.	2013	(*148*)

Table S3. Tabulated data that is depicted in Figure 4.

	Present	MIS 5e	MIS 11	Pliocene
Age	2014 A.D.	~125 ka	~400 ka	~3.3 Ma
Global mean temperature (°C) (1)	**1** (3)	~1 (7)	1 to 2? (12)	1.9 to 3.6 (16)
Arctic temperature (°C) (1)	**2** (4)	**4 to 8** (8)	**4 to 9** (13)	**4 to 11** (17)
Antarctic temperature (°C) (1)	? (5)	**4 to 5** (9)	**2 to3** (14)	?
Peak Atmospheric CO_2 (ppm)	**397** (5)	**287** (10)	**286** (10)	**350 to 450** (18)
Peak sea level (m) (2)	**0** (6)	**6 to 9** (11)	**6 to 13** (15)	*>6* (19)

Bold = data; Normal font = data and modeling; *Italics* = hypothesized

Footnotes:

(1) Temperatures are rounded to the nearest degree and reported relative to the pre-Industrial period. Please refer to primary sources for definitions of the pre-Industrial baseline in each study.

(2) Sea level is rounded to the nearest meter, and reported relative to the pre-Industrial period.

(3) Observed global mean land-ocean surface temperature; from Figure SPM1a in Ref. (*149*).

(4) For the area 60-90 °N, relative to 1900 AD, Ref. (*150*); Data from the CRUTEM4v dataset, which is available at www.cru.uea.ac.uk/cru/data/temperature/.

(5) Instrumental data do not extend to pre-industrial period, and there is low confidence in trends since the late 1950s (*79*).

(5) Globally averaged marine surface annual mean data, observed in 2014 Ref. (*151*).

(6) Present global mean sea level is rounded to the nearest whole number.

(7) Global mean land-ocean surface temperature; Ref. (*58, 68, 152*)

(8) Refs (*59, 60, 153*).

(9) Antarctic ice cores, Ref. (*153*)

(10) Antarctic ice cores, Ref. (*39*)

(11) Refs. (*61-64, 77*) and this study

(12) Refs (*36-38*).

(13) Refs. (*40, 41*). Based on only 2 records; data is much more limited than for MIS 5e.

(14) Antarctic ice core, Ref. (*42*).

(15) Ref. (*51-53*)

(16) Ref. (*16*)

(17) Ref. (*17*) Data from 5 sites.

(18) Refs (*14, 15*).

(19) Hypothesis from this study.

Table S4. Sources of sea level data shown in Figure 4.

Source notation in figure	**Study**	**Year**	**Bibliography number**
K09	Kopp et al.	2009	(*62*)
DL12	Dutton and Lambeck	2012	(*61*)
O13	O'Leary et al	2013	(*64*)
D15	Dutton et al.	2015	(*63*)
G12	Grant et al.	2012	(*65*)
SR09	Sosdian and Rosenthal	2009	(*31*)
E12	Elderfield et al.	2012	(*54*)
RM12	Raymo and Mitrovica	2012	(*51*)
R12	Roberts et al.	2012	(*52*)
C15	Chen et al.	2014	(*53*)
R09	Rohling et al.	2009	(*55*)
M12	Miller et al.	2012	(*24*)

Table S5. Data sources for figure S1.

Source #	**Study**	**Year**	**Bibliography number**
1	Broecker and Van Donk	1970	(*154*)
2	CLIMAP 1976	1976	(*155*)
3	CLIMAP 1981	1981	(*156*)
4	Chappell and Shackleton	1986	(*134*)
5	Nakada and Lambeck	1988	(*157*)
6	Fairbanks	1989	(*158*)
7	Tushingham and Peltier	1991	(*112*)
8	Peltier	1994	(*159*)
9	Hanebuth et al	2000	(*160*)
10	Yokoyama et al	2001	(*161*)
11	Yokoyama et al.	2000	(*162*)
12	Lambeck and Chappell	2001	(*163*)
13	Clark and Mix: EPILOG	2002	(*164*)
14	Lambeck et al.	2002	(*165*)
15	Milne et al.	2002	(*166*)
16	Peltier	2002	(*167*)
17	Peltier	2004	(*126*)
18	Peltier and Fairbanks	2006	(*168*)
19	Hanebuth et al.	2009	(*169*)
20	Clark et al.	2009	(*170*)
21	Clark et al.	2012	(*171*)
22	Austermann et al.	2013	(*98*)
23	Lambeck et al.	2014	(*82*)

References

127. A. J. Long, D. H. Roberts, S. Dawson, Early Holocene history of the west Greenland Ice Sheet and the GH-8.2 event. *Quaternary Science Reviews* **25**, 904 (2006).
128. B. Horton *et al.*, Influence of tidal-range change and sediment compaction on Holocene relative sea-level change in New Jersey, USA. *Journal of Quaternary Science* **28**, 403 (2013).
129. M. P. Hijma, K. M. Cohen, Timing and magnitude of the sea-level jump preluding the 8200 yr event. *Geology* **38**, 275 (2010).
130. Y. Zong, Mid-Holocene sea-level highstand along the Southeast Coast of China. *Quaternary International* **117**, 55 (2004).
131. C. D. Woodroffe, H. V. McGregor, K. Lambeck, S. G. Smithers, D. Fink, Mid-Pacific microatolls record sea-level stability over the past 5000 yr. *Geology* **40**, 951 (2012).
132. K. Lambeck, in *Glacial Isostatic Adjustment and the Earth System,* J. X. Mitrovica, B. Vermeersen, Eds. (American Geophysical Union, 2002), pp. 33-50.
133. H. H. Veeh, Th^{230}/U^{238} and U^{234}/U^{238} ages of Pleistocene high sea level stand. *Journal of Geophysical Research* **71**, 3379 (1966).
134. J. Chappell, N. J. Shackleton, Oxygen isotopes and sea level. *Nature* **324**, 137 (1986).
135. D. Muhs, Evidence for the Timing and Duration of the Last Interglacial Period from High-Precision Uranium-Series Ages of Corals on Tectonically Stable Coastlines. *Quaternary Research* **58**, 36 (2002).
136. D. R. Muhs, K. R. Simmons, B. Steinke, Timing and warmth of the Last Interglacial period: new U-series evidence from Hawaii and Bermuda and a new fossil compilation for North America. *Quaternary Science Reviews* **21**, 1355 (2002).
137. K. M. Cuffey, S. J. Marshall, Substantial contribution to sea-level rise during the last interglacial from the Greenland ice sheet. *Nature* **404**, 591 (2000).
138. P. Huybrechts, Sea-level changes at the LGM from ice-dynamic reconstructions of the Greenland and Antarctic ice sheets during the glacial cycles. *Quaternary Science Reviews* **21**, 203 (2002).
139. L. Tarasov, W. R. Peltier, Greenland glacial history, borehole constraints, and Eemian extent. *Journal of Geophysical Research* **108**, 2143 (2003).
140. N. L'homme, G. K. C. Clarke, S. J. Marshall, Tracer transport in the Greenland Ice Sheet: constraints on ice cores and glacial history. *Quaternary Science Reviews* **24**, 173 (2005).
141. B. L. Otto-Bliesner *et al.*, Simulating Arctic climate warmth and icefield retreat in the Last Interglacial. *Science* **311**, 1751 (2006).
142. J. Oerlemans, D. Dahl-Jensen, V. Masson-Delmotte, Ice sheets and sea-level rise. *Science* **313**, 1043 (2006).
143. A. Robinson, R. Calov, A. Ganopolski, Greenland Ice Sheet model parameters constrained using simulations of the Eemian Interglacial. *Climate of the Past Discussions* **6**, 1551 (2011).
144. J. G. Fyke *et al.*, A new coupled ice sheet/climate model: description and sensitivity to model physics under Eemian, Last Glacial Maximum, late Holocene and modern climate conditions. *Geoscientific Model Development* **4**, 117 (2011).

145. A. Born, K. H. Nisancioglu, Melting of Northern Greenland during the last interglaciation. *The Cryosphere* **6**, 1239 (2012).
146. A. Quiquet, C. Ritz, H. J. Punge, D. Salas y Melia, Greenland ice sheet contribution to sea level rise during the last interglacial period: a modelling study driven and constrained by ice core data. *Climate of the Past* **9**, 353 (2013).
147. M. M. Helsen, W. Van de Berg, R. S. W. van de Wal, M. R. van den Broeke, J. Oerlemans, Coupled regional climate-ice sheet simulation shows limited Greenland ice loss during the Eemain. *Climate of the Past Discussions* **9**, 1735 (2013).
148. E. J. Stone, D. J. Lunt, J. D. Annan, J. C. Hargreaves, Quantification of Greenland ice-sheet contribution to Last Interglacial sea-level rise. *Climate of the Past* **9**, 621 (2013).
149. L. V. Alexander *et al.*, in *The Physical Science Basis. Contribution of Working Group I to the Fifth Assessment Report of the Intergovernmental Panel on Climate Change* T. F. Stocker *et al.*, Eds. (Cambride University Press, Cambridge, 2013), pp. 3-29.
150. J. Overland *et al.*, in *Arctic Report Card: Update for 2014*. (2014).
151. P. Tans, R. Keeling, in *Global Greenhouse Gas Reference Network*. (NOAA/ESRL, 2015).
152. C. S. M. Turney, R. T. Jones, Does the Agulhas Current amplify global temperatures during super-interglacials? *Journal of Quaternary Science* **25**, 839 (2010).
153. E. Capron *et al.*, Temporal and spatial structure of multi-millennial temperature changes at high latitudes during the Last Interglacial. *Quaternary Science Reviews* **103**, 116 (2014).
154. W. S. Broecker, J. van Donk, Insolation changes, ice volumes, and the O18 record in deep-sea cores. *Reviews of Geophysics* **8**, 169 (1970).
155. CLIMAP Project Members, The surface of the ice-age Earth. *Science* **191**, 1131 (1976).
156. CLIMAP Project Members, in *Chart Series MC-36*. (Geological Society of America, 1981).
157. M. Nakada, K. Lambeck, The melting history of the late Pliestocene Antarctic Ice Sheet. *Nature* **333**, (1988).
158. R. G. Fairbanks, A 17,000-year glacio-eustatic sea level record: influence of glacial melting rates on the Younger Dryas event and deep-ocean circulation. *Nature* **342**, 637 (1989).
159. W. R. Peltier, Ice age paleotopography. *Science* **265**, 195 (1994).
160. T. Hanebuth, K. Stattegger, P. M. Grootes, Rapid Flooding of the Sunda Shelf: A Late-Glacial Sea-Level Record. *Science* **288**, 1033 (2000).
161. Y. Yokoyama, P. De Deckker, K. Lambeck, P. Johnston, L. K. Fifield, Sea-level at the Last Glacial Maximum: evidence from northwestern Australia to constrain ice volumes for oxygen isotope stage 2. *Palaeogeography, Palaeoclimatology, Palaeoecology* **165**, 281 (2001).
162. Y. Yokoyama, K. Lambeck, P. De Deckker, P. Johnston, L. K. Fifield, Timing of the Last Glacial Maximum from observed sea-level minima. *Nature* **406**, 713 (2000).
163. K. Lambeck, J. Chappell, Sea level change through the last glacial cycle. *Science* **292**, 679 (2001).
164. P. U. Clark, A. C. Mix, Ice sheets and sea level of the Last Glacial Maximum. *Quaternary Science Reviews* **21**, 1 (2000).

165. K. Lambeck, Y. Yokayama, T. Purcell, Into and out of the Last Glacial Maximum: sea-level change during Oxygen Isotope Stage 3 and 2. *Quaternary Science Reviews* **21**, 343 (2002).
166. G. A. Milne, J. X. Mitrovica, D. P. Schrag, Estimating past continental ice volume from sea-level data. *Quaternary Science Reviews* **21**, 361 (2002).
167. W. R. Peltier, On eustatic sea level history: Last Glacial Maximum to Holocene. *Quaternary Science Reviews* **21**, 377 (2002).
168. W. R. Peltier, R. G. Fairbanks, Global glacial ice volume and Last Glacial Maximum duration from an extended Barbados sea level record. *Quaternary Science Reviews* **25**, 3322 (2006).
169. T. Hanebuth, K. Stattegger, A. Bojanowski, Termination of the Last Glacial Maximum sea-level lowstand: The Sunda-Shelf data revisited. *Global and Planetary Change* **66**, 76 (2009).
170. P. U. Clark *et al.*, The Last Glacial Maximum. *Science* **325**, 710 (2009).
171. P. U. Clark *et al.*, Global climate evolution during the last deglaciation. *Proceedings of the National Academy of Sciences* **109**, E1134 (2012).